Disentangled cascade adaptive optics for the SPHERE instrument forthcoming upgrade

Nicolas Galland, Henri Francois Raynaud, Markus Kasper, Charles Goulas, Clémentine Béchet, Florian Ferreira, Michel Tallon, Fabrice Vidal, Maud Langlois, Anthony Boccaletti, et al.

AO4ELT7 - June 2023 - Avignon

Disentangled cascade adaptive optics for the SPHERE instrument forthcoming upgrade

N. Galland[a], H.-F. Raynaud[a], M. Kasper[i], C. Goulas[b], C. Béchet[c], F. Ferreira[b], M. Tallon[c], F. Vidal[b], M. Langlois[c], A. Boccaletti[b], G. Chauvin[d], E. Diolaiti[e], R. Gratton[f], M. Loupias[c], J. Milli[g], F. Wildi[h], and C. Kulcsár[a]

[a]Université Paris-Saclay, Institut d'Optique Graduate School, CNRS, Laboratoire Charles Fabry, 91127 Palaiseau, France
[b]LESIA, Observatoire de Paris, CNRS, Université Paris Diderot, Université Pierre et Marie Curie, 5 place Jules Janssen, 92190 Meudon, France
[c]Univ Lyon, Univ Lyon1, Ens de Lyon, CNRS, Centre de Recherche Astrophysique de Lyon UMR5574, F-69230, Saint-Genis-Laval, France
[d]Laboratoire Lagrange, Université Côte d'Azur, CNRS, Observatoire de la Côte d'Azur, 06304 Nice, France
[e]INAF - Osservatorio di Astrofisica e Scienza dello Spazio (OAS), via Gobetti 93/3, 40129 Bologna, Italy
[f]INAF - Osservatorio Astronomico di Padova (OAPd), Vicolo dell'Osservatorio 5, 35122 Padova, Italy
[g]Université Joseph Fourier-Grenoble 1/CNRS-INSU, Institut de Planétologie et d'Astrophysique de Grenoble (IPAG), 414 rue de la Piscine, Saint Martin d'Heres, France
[h]Observatoire de Geneve, Ch Pegasi 51, CH-1290 Sauverny, Switzerland
[i]European Southern Observatory, Garching bei München, Germany

Corresponding author: N. Galland, E-mail: nicolas.galland@institutoptique.fr

ABSTRACT

The Spectro-Polarimetric High-contrast Exoplanet REsearch instrument (SPHERE) is a European Southern Observatory (ESO) exoplanet imaging instrument installed on the 8m Very Large Telescope at Paranal (Chile). The results obtained during 8 years of operation since its commissioning in 2014 have encouraged ESO to define new science objective and thus to develop an upgrade of the instrument withing the SPHERE+ project. Considering the predominant role of adaptive optics (AO) for high contrast imaging and coronography, it has been decided to update the AO system of SPHERE by adding a 2^{nd} stage of correction that will take as an input the residual wavefront from the 1^{st} stage. This article presents some control developments for this 2^{nd} AO stage, including specific issues induced by the two-stage approach. We investigate a particular solution to address the problem of a non stochastic signal arising from the oversampling of the 1^{st} stage residue.

Keywords: Adaptive Optics, XAO, Cascade AO systems, Disentangled AO

1. INTRODUCTION

The SPHERE (Spectro-Polarimetric High-contrast Exoplanet REsearch) instrument is a coronographic imager for the VLT facility dedicated to exoplanet imaging and spectroscopy in operation since 2015 [1]. This instrument already benefits from an extreme adaptive optics system called SAXO (SPHERE AO for eXoplanet Observation, [8]). Exoplanet imaging relies on image quality, and coronographic observation requires very good image stability. These requirements have been well provided by SAXO.

Considering the results already achieved over 8 years, it has been decided to define new science objectives through an upgrade of the instrument within the SPHERE+ consortium. As a part of this upgrade, the AO system will also be upgraded to improve image quality and coronographic performance.

2. CASCADE AO SYSTEM

The solution selected for the SAXO upgrade is the addition of a 2^{nd} AO system (called SAXO+) at the output of the 1^{st} stage SAXO. The 2^{nd} stage will take as input the 1^{st} stage residual phase. This kind of two-stage setup is called Cascade Adaptive Optics (CAO). The main advantage of such an implementation is that it leaves the first system untouched and allows to increase performance without incurring the cost of changing the whole system [10]. One of the main interests of this 2^{nd} stage is that it may operate at a different (generally higher) sampling frequency, thus enabling to compensate for higher frequency components of either the turbulence or other perturbation sources, such as vibrations and windshake. On the other hand, this requires to take care of possible effects that may arise when two different AO sampling frequencies are used.

2.1 Foreseen implementation for SPHERE+ AO control

The focus of this paper is to introduce some contributions to SAXO+ control. The instrument is still in design phase, but figure 1 shows some foreseen characteristics of this two-stage system in the form of a block diagram. The implementation presented in this figure is called *standalone mode*, with each stage having its own Real Time Controller (RTC). An integrated solution with a single AO loop is also under study, with for example the 2^{nd} stage RTC receiving measurements from both WaveFront Sensors (WFSs) and sending commands to the Deformable Mirror (DM) and to the Tip-Tilt Mirror (TTM) of the 1^{st} stage and also to the DM of the 2^{nd} stage.

The 2^{nd} stage is expected to run with a Pyramid WFS and a fast DM with a total number of actuators in the range of 500 to 1000. The RTC for this 2^{nd} stage will be based on the COSMIC platform (see for example [5]) in order to benefit from the speed of GPU computation.

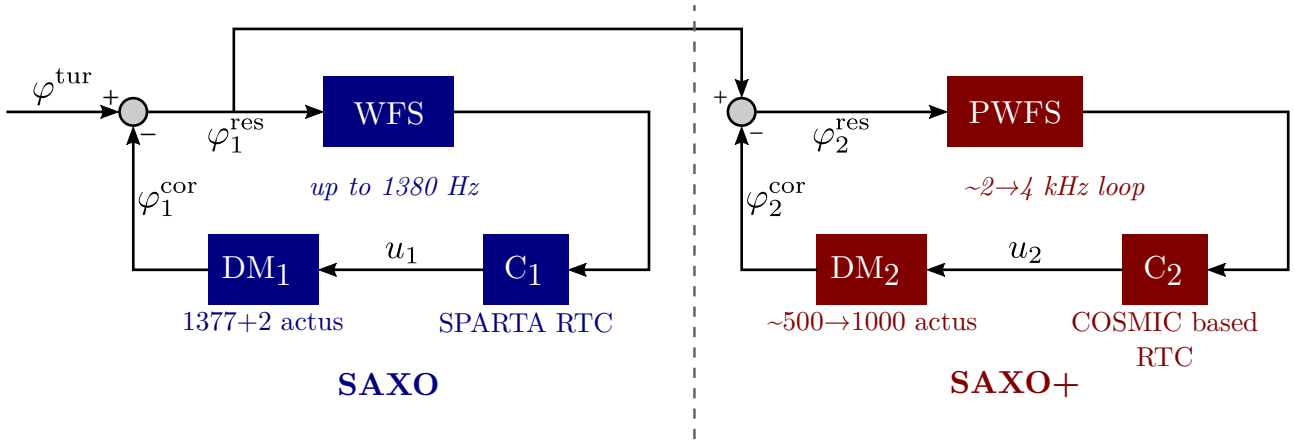

Figure 1. Two-stage CAO setup for SPHERE+, showing dimensional features of the existing system (SAXO) and of the foreseen 2nd stage (SAXO+).

2.2 Challenges of CAO systems

The main advantage of such two-stage systems is that the fast 2nd stage is able to compensate for perturbations with higher temporal frequencies which cannot be efficiently sensed and corrected by the 1st stage. However, the combination of two different sampling frequencies can lead to unwanted effects.

The residual phase entering the 2nd stage corresponds to the residual of the 1st stage, which runs more slowly. The 1st stage residual phase enters the faster 2nd stage and will be thus oversampled. This generates spurious high-frequency oscillations which are hardly compensated by any 2nd stage linear time-invariant controller. Such effect can be seen in the results presented later on in figure 4 where the modal temporal trajectories for KL mode 1 are displayed. On the left hand (CAO case) are shown the turbulent KL mode 1 (its opposite value is shown to ease curves comparison), the 1st stage correction and the total correction. The latter exhibits strong high frequency variations that are due to the oversampling of the 1st stage residuals. Indeed, the 1st stage outputs see-saw-like signals as noted in [10].

This kind of behaviour can under some circumstances degrade the overall performance level of the system, but it is also problematic if one wants to use a predictive control law that would rely on data driven model identification of the global incoming turbulence, as we plan to test for this system. Indeed, such identification schemes, based on machine learning, have been proven to be very efficient on sky [9] and are also being developed for unsupervised predictive control within the H2020 ORP project [6, 7].

3. DISENTANGLED CAO

The spurious see-saw-like signals entering the 2nd stage can be compensated using the disentangled CAO (dCAO) control scheme presented in figure 2. The basic idea is to subtract from the 2nd stage control C_2 (which operates as if it were alone) the predicted effect of the 1st stage correction. When the dCAO compensation at the bottom of figure 2 is activated (that is when the projection of u_1 commands is used), the sum of the 1st and 2nd stage corrections becomes equivalent to the correction which would have been generated by a standalone 2nd stage using the same controller C_2. This results in a kind of off-load arrangement, where the faster (and hence potentially more effective) 2nd stage standalone control effort u_2^{ctrl} is effectively split between the two stages, allowing to use a 2nd stage DM with high bandwidth but limited stroke. This approach allows to compensate for the effect of the oversampled 1st stage correction [2].

However, implementing the dCAO scheme requires two things. First, the 1st stage commands need to be projected onto the actuator space of the 2nd stage and a special care must be taken to construct the projection matrix. Second, one must carefully account for the respective delays of both stages, in order to properly synchronize the dCAO compensation. The compensation scheme does not change in case of a fractional loop

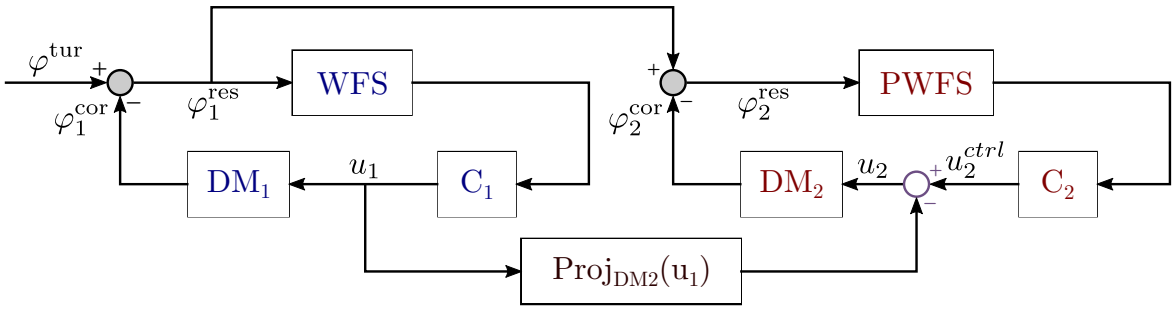

Figure 2. Block diagram of a dCAO setup. The commands from the 1st stage are projected onto the 2nd stage DM basis (it can be either zonal or modal) and subtracted from the commands calculated by the 2nd stage controller.

delay for the 1st stage, the difference of the loop delays has simply to be accounted for. In the case where the 2nd stage exhibits a fractional loop delay, the compensation scheme has to be slightly modified. In this article, we have considered that each loop has an integer loop delay of 2 frames, the case of fractional loop delays being left for future work.

4. SIMULATION RESULTS

4.1 Simulation framework and parameters

Within the SPHERE+ consortium, AO end-to-end simulations are mainly performed using the COMPASS framework [4]. However, dealing with the dCAO was not straightforward at the time we were performing the first performance tests. To take advantage of previous work done with dCAO such as the ones presented in [10], we decided to use an OOMAO-based simulation under MATLAB. OOMAO stands from *Object-Oriented Matlab for Adaptive Optics* and is a MATLAB toolbox that is widely used for AO simulations [3].

Due to implementation characteristics, a few changes have been made in the simulation parameters. The 1st stage is replicated with the exact number of actuators for the HODM (1377), but our simulation does not include a separated tip-tilt mirror. Concerning the WFS, the number of valid subapertures is slightly different, with 1197 in our simulation to be compared to 1240 in the reference cases. Regarding the 2nd stage, the number of equivalent subapertures for the pyramid wavefront sensor has been set to 50 across the pupil, which gives the same number of valid subapertures than what COMPASS uses. However, the centroiding method is different. While COMPASS uses a "masked pixel" algorithm where the intensity of all valid pixels for the 4 sub-images are concatenated, OOMAO computes x and y slopes from the pyramid measurements. As a consequence, the total number of measurements is 8064 in COMPASS and 4032 in OOMAO. Concerning the DM, the exact number of actuators has not been chosen yet within the consortium, so our OOMAO simulations are using 540 actuators for the 2nd stage (26 actuators accross the pupil) which is in the range of possibilities for the actual SAXO+ DM.

From a control point of view, both stages are using a standard integrator control law. The commands are directly calculated in the modal basis and a filtering is done so that the number of controlled KL modes is 800 for the 1st stage and 200 for the 2nd stage.

4.2 Performance comparison

Using the framework described above, we performed simulations with both regular CAO and dCAO controller, based on integrator controllers for both stages. For each performance index that we considered, the simulation has been performed in two configurations: the first case uses the frequency pair (1 kHz, 2 kHz) for 1st and 2nd stage loops, and the second configuration uses (1 kHz, 4 kHz). The global Fried parameter is $r_0 = 15.7$ cm. The C_n^2 profile is that of ESO with 35 layers and median wind profile. The magnitudes are 7.41 in I band for the 1st

stage WFS and 5.35 in J band for the 2nd stage WFS. The scientific camera is in H band (1.45-1.8 µm), where contrasts and Strehl ratios (SR) are computed.

If we consider the SR averaged over 1000 iterations, we notice that the variation is within one point of SR. The SR derived from the 1st stage residual phase is 88%, and after the 2nd stage, it varies between 91.5% and 92.5% depending on the frequency and the controller we use.

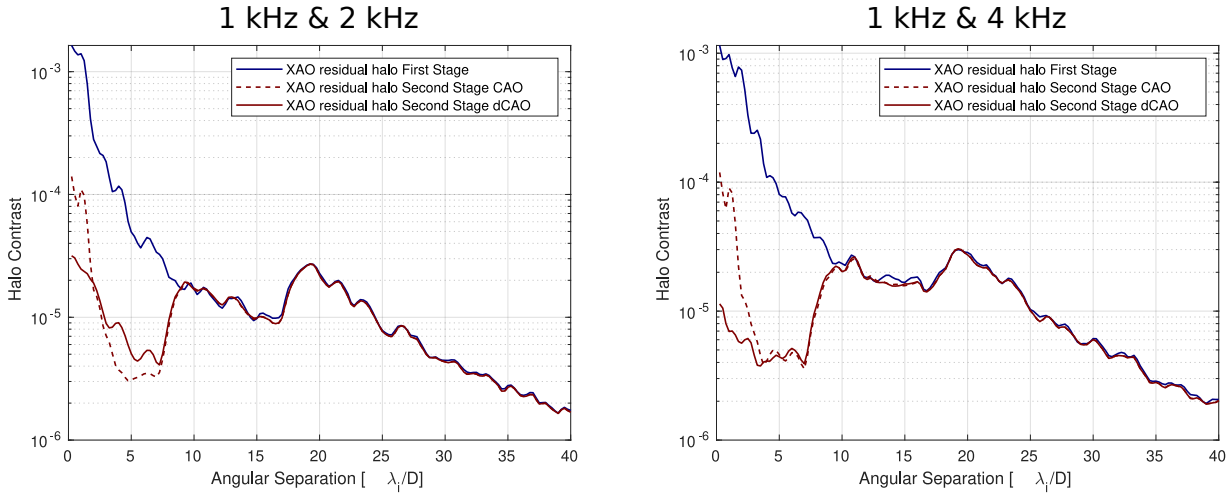

Figure 3. Residual halo contrast curves estimated in closed-loop for both frequencies configurations and with CAO (red dashed line) and dCAO (red plain line). The contrast obtained with the 1st stage only is also displayed (blue plain line).

However, the effect on the coronagraphic contrast is more significant. The figure 3 displays 1st and 2nd stage residual halo contrast for the two frequency configurations with CAO and dCAO. When the frequency of the 2nd stage is 4 kHz, the contrast below $4\lambda/D$ is significantly better (up to one order of magnitude below $2\lambda/D$). However, with the 2nd stage running at 2 kHz, the contrast is better below $2\lambda/D$ and shows a small degradation at higher separations above $4\lambda/D$.

One explanation for this degradation is the fact that the dCAO implementation reduces the low temporal frequency performance as the cost of a better compensation of high frequencies. With a 4 to 1 ratio, the improvement at high frequencies is good enough to positively impact the overall quality of the correction. On the other hand, when the 2nd stage is only two times faster than the 1st stage, this increase is no longer sufficient to compensate for the loss at low frequencies for the observation conditions considered here.

An interesting behaviour is however given by the modal time trajectories of turbulence and computed commands for 1st and 2nd stages as illustrated in figure 4. The modal basis that has been used to represent the different phases as well as compute the command vector is the Kahrunen-Loéve basis of the HODM, and the plots are done for the first mode of the KL basis.

We can see from these simulations that the dCAO total correction trajectories are far smoother than that of the CAO commands. As expected, the dCAO scheme allows for a good compensation of the high-frequency oscillations.

5. CONCLUSION AND PERSPECTIVES

Our simulations have confirmed that the residual phase of the 1st stage AO correction generates high frequencies components in the 2nd stage correction. However, the dCAO scheme that we have presented here allows to compensate for that. In addition to a potentially better contrast, other observation conditions need to be explored from the contrast point of view, this method also enables to obtain smoother time trajectories of the modal component of the total correction performed by the two stages. This is especially interesting if one wants to implement a predictive controller for the 2nd stage: when working in standard CAO mode, the prediction model

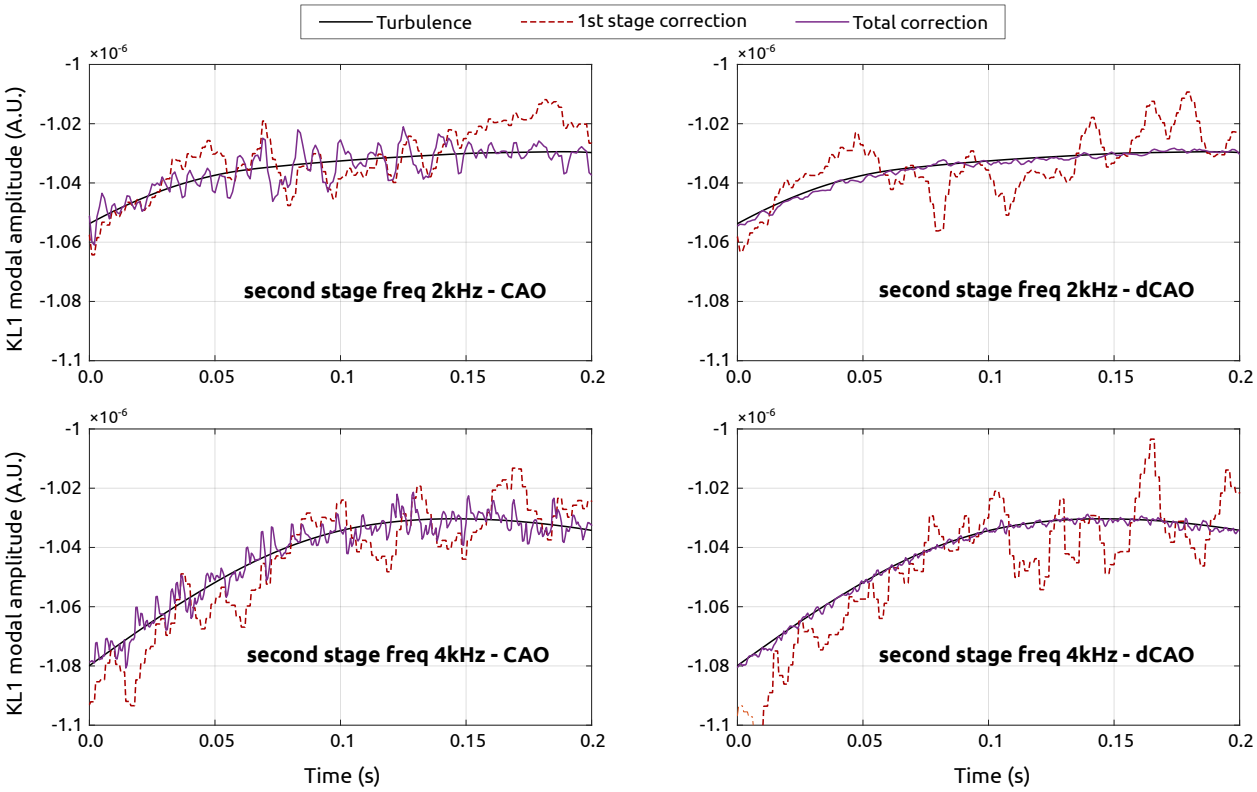

Figure 4. Temporal trajectories of first mode from the KL basis of the HODM in presence of turbulence (black), 1st stage correction (dashed red) and total correction (purple) for 2 frequency configurations (2 kHz and 4 kHz for SAXO+, the 1st stage running at 1 kHz), for CAO (left) and dCAO (right).

has to be identified from time trajectories of the 1st stage residuals, which is a non-stationary stochastic process that generates high frequencies in the faster 2n stage. Conversely, with dCAO, the 2nd stage regulator is effectively computing a correction suited to the global incoming turbulent phase as if it were alone. As a consequence, model identification can be performed on much smoother trajectories. This is a better situation for model identification, thus leading to more robust and accurate prediction. The future work we envision for this project is the implementation of such predictive controllers with dCAO in presence of fractional delays in both loops.

Acknowledgement

This work has received funding from the European Union's Horizon 2020 Research and Innovation Programme under grant agreement No 101004719.

References

[1] Beuzit, Jean-Luc et al. "SPHERE: the exoplanet imager for the Very Large Telescope". In: *A&A* 631 (2019), A155. DOI: 10.1051/0004-6361/201935251. URL: https://doi.org/10.1051/0004-6361/201935251.

[2] Nelly Natalia Cerpa Urra. "Advanced Control Laws for Exoplanet Imaging Adaptative Optics". PhD thesis. Université' Paris-Saclay, Institut d'Optique Graduate School, CNRS, Laboratoire Charles Fabry, 2022.

[3] Rodolphe Conan and Carlos Correia. "Object-oriented Matlab adaptive optics toolbox". In: *Adaptive Optics Systems IV*. Ed. by Enrico Marchetti, Laird M. Close, and Jean-Pierre Véran. Vol. 9148. International Society for Optics and Photonics. SPIE, 2014, p. 91486C. DOI: 10.1117/12.2054470. URL: https://doi.org/10.1117/12.2054470.

[4] Florian Ferreira et al. “COMPASS: An Efficient GPU-based Simulation Software for Adaptive Optics Systems”. In: *2018 International Conference on High Performance Computing & Simulation (HPCS)*. 2018, pp. 180–187. DOI: 10.1109/HPCS.2018.00043.

[5] Florian Ferreira et al. “Hard real-time core software of the AO RTC COSMIC platform: architecture and performance”. In: *Adaptive Optics Systems VII*. Ed. by Laura Schreiber, Dirk Schmidt, and Elise Vernet. Vol. 11448. International Society for Optics and Photonics. SPIE, 2020, p. 1144815. DOI: 10.1117/12.2561244. URL: https://doi.org/10.1117/12.2561244.

[6] Tim Morris et al. “The ORP on-sky community access program for adaptive optics instrumentation development”. In: *Adaptive Optics Systems VII*. Vol. 11448. SPIE. 2020, pp. 1072–1078.

[7] Timothy J. Morris et al. “On-sky telescope access for instrument development”. In: *Adaptive Optics Systems VIII*. Ed. by Laura Schreiber, Dirk Schmidt, and Elise Vernet. Vol. 12185. International Society for Optics and Photonics. SPIE, 2022, p. 1218510. DOI: 10.1117/12.2630243. URL: https://doi.org/10.1117/12.2630243.

[8] Cyril Petit et al. “SPHERE eXtreme AO control scheme: final performance assessment and on sky validation of the first auto-tuned LQG based operational system”. In: *Adaptive Optics Systems IV*. Ed. by Enrico Marchetti, Laird M. Close, and Jean-Pierre Véran. Vol. 9148. International Society for Optics and Photonics. SPIE, 2014, 91480O. DOI: 10.1117/12.2052847. URL: https://doi.org/10.1117/12.2052847.

[9] Baptiste Sinquin et al. “On-sky results for adaptive optics control with data-driven models on low-order modes”. In: *Monthly Notices of the Royal Astronomical Society* 498.3 (Oct. 2020), pp. 3228–3240. ISSN: 0035-8711. DOI: 10.1093/MNRAS/STAA2562. URL: https://academic.oup.com/mnras/article/498/3/3228/5897378.

[10] Nelly Natalia Cerpa Urra et al. “Cascade adaptive optics: contrast performance analysis of a two-stage controller by numerical simulations”. In: *Journal of Astronomical Telescopes, Instruments, and Systems* 8.1 (2022), p. 019001. DOI: 10.1117/1.JATIS.8.1.019001. URL: https://doi.org/10.1117/1.JATIS.8.1.019001.